Characterization of Alumina-Supported Model Catalysts Using Positronium Lifetime Technique

J. Lahtinen* and P. Hautojärvi

Laboratory of Physics, Helsinki University of Technology, 02150 Espoo, Finland

Received: August 30, 1996; In Final Form: October 24, 1996[⊗]

The sensitivity of positronium to detect inner surfaces of porous material has been utilized to study model catalysts of Pt, Co, and Ni on γ-alumina. The results indicate that a carrier material with higher surface area can be distinguished from a lower surface area carrier. The technique is very sensitive to small amounts (0.01%) of metal particles on the catalyst surface. The difference between the state of reduction in the model catalysts is clearly visible between Pt and Co catalysts. Monte-Carlo simulations are used to model the behavior of positronium in porous material.

Introduction

The catalyst activity of alumina-supported catalysts is an unresolved combination of the properties of the carrier and the impregnated metal. It is difficult to obtain direct information on the internal surfaces of porous materials. Standard surface characterization methods, like XPS, can detect only a very small fraction of the active area of a supported catalyst. The internal surfaces can be detected, for example, by methods where photons are used to carry the information to the detection system. Infrared and Mössbauer spectroscopies are the most widely used methods applied to this field.[1]

Positron annihilation spectroscopy (PAS) is another in-situ surface sensitive method that can be used to probe the properties of the internal surfaces of porous catalysts. Traditionally, PAS is successfully applied to investigate electronic structure and open volume defects in materials,[2,3] but recently it has been introduced also to the catalysis studies as discussed by Lahtinen and Vehanen,[4] Cheng et al.,[4] and Schrader and Jean.[6]

In PAS, high-energy positrons from a radioactive isotope are directly implanted into the studied sample. During slowing down in porous material, a positron may capture an electron to form a hydrogen-like bound state, positronium (Ps). The spin singlet state (para, p-Ps) suffers a rapid self-annihilation with a lifetime of 125 ps. In the spin triplet state (ortho, o-Ps) the 2γ self-annihilation is forbidden, and the o-Ps lives long enough to enter a cavity. Inside the cavity the o-Ps is bouncing from wall to wall until it hits a chemically active site, giving rise to a pick-off annihilation. This technique has been applied to study, for example, the cage size,[7] the acidity,[8] and the adsorption of O_2 and NO[9] on zeolites. The reactivity of o-Ps with different transition metals has been studied on γ-alumina[10,11] as well as the adsorption of H_2 on Fe/SiO_2[12] and air on Fe/Al_2O_3.[13]

The o-Ps formed inside the sample can be detected by measuring the lifetime and the relative intensity of the long lifetime component of the annihilation radiation. The lifetime of the o-Ps in the 3γ annihilation in vacuum is 142 ns, but it can be shortened by the pick-off annihilation, where the positron in the o-Ps atom interacts with a spin-opposite electron, causing the 2γ annihilation. In an environment where the electron density is very small, like inside the internal voids of oxide powders, the o-Ps lifetime is nearly as long as in the vacuum.

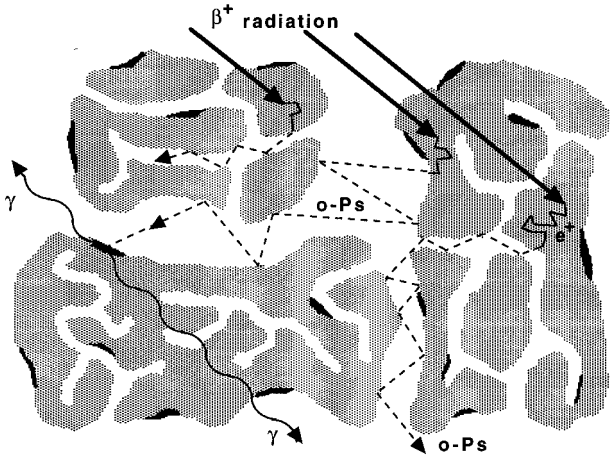

Figure 1. Schematic drawing explaining the positron lifetime experiment. Positrons emitted from a radioactive source slow down inside the catalyst, and some of them are emitted out from the alumina grains as ortho-positronium atoms (o-Ps). The o-Ps atoms annihilate when they hit free electrons available in metal particles (black areas).

During its lifetime the o-Ps atom travels a distance of several millimeters in the internal pores, but it cannot repenetrate the oxide grains. The information is obtained as an average over all the surfaces of the sample, in contrast to the external surface detected by electron spectroscopies. The schematic picture of the experiment is given in Figure 1, where the gray area represents alumina grains and the black area the catalyst metal. Once positrons have been annihilated inside the porous material, information on the environment is conveyed by γ-quanta emitted in the annihilation process. The positron is sensitive to changes caused by metal deposition, by adsorption, or by formation of chemical compounds on the internal surfaces, processes that are of great interest in catalysis research.[4,5]

We report o-Ps lifetime measurements in Pt/Al_2O_3, Co/Al_2O_3, and Ni/Al_2O_3 model catalysts with metal loadings from 3 ppm to 10%. Also different alumina carrier materials were studied without additional metal loading. Positrons are reflected very effectively from the carrier material, whereas collisions with metallic particles speed up the annihilation. The results indicate that a very small amount (0.03%) of metallic Pt is able to fully quench the o-Ps signal. In the case of less noble Co and Ni the minimum amount of metal introducing changes in the o-Ps signal is about 0.1%. Monte-Carlo simulations indicate that the o-Ps annihilation probability per collision with the carrier material is on the order of 10^{-7} and that with a metallic particle

* Email: Jouko.Lahtinen@hut.fi. FAX: +358-9-451 3116.

[⊗] Abstract published in *Advance ACS Abstracts,* February 1, 1997.

S1089-5647(96)02638-7 CCC: $14.00

TABLE 1: Properties of the Different Carrier Materials and the Measured Positronium Lifetimes $\tau_{o\text{-}Ps}$ and Their Intensities $I_{o\text{-}Ps}$

carrier	material	surface area (m^2/g)	pore volume (cm^2/g)	Ps signals $\tau_{o\text{-}Ps}$ (ns)	Ps signals $I_{o\text{-}Ps}$ (%)
Al-0104	Al_2O_3	100	0.38	92	20
Al-4912	Al_2O_3	200	0.96	58	23
Al-01020	Al_2O_3	200		49	22

is $10^{-5}-10^{-3}$ depending on the degree of reduction. The concentration dependence of the o-Ps lifetime spectra was also simulated, and it reproduced well the measured data.

Experimental Section

The carrier materials used in the experiments, Al-0104 T 1/8″, Al-4192, and Al-0120, were obtained from Harshaw. The Brunauer−Emmet−Teller surface areas of the carriers were 200 m^2/g except in Al-0104, where it was only 100 m^2/g. Table 1 gives a summary of the carrier materials.

The metal-containing samples were obtained from the Chemical Laboratory of the State Research Center of Finland. They had been prepared by impregnation of chloride precursors on two different kinds of alumina carriers (Al-0104 and Al-0120). The metal concentrations in the catalysts were between 3 and 10^5 wt ppm. All samples were dried, calcined in air at 773 K for 3−5 h, and reduced at 693 K (673 K for Pt) in flowing hydrogen for 3 h before the experiments.

Figure 2 shows the schematic view of the experimental apparatus. The sample chamber was a stainless steel tube with ConFlat flanges. The system was pumped with an oil-diffusion pump and a liquid-nitrogen-cooled cold trap down to 10 μPa pressures. The vacuum diagnostics system consisted of a residual gas analyzer and a Pirani-Penning gauge. For reduction and chemisorption experiments a gas-handling manifold was attached to give controlled exposures of different gases.

The sample cell was a 14 mm diameter tube made of aluminum−bronze, closed on both ends with a stainless steel mesh with 56 × 56 μm holes to allow gas flow and to prevent the catalyst grains from escaping. The sample temperature was varied with the heater block from room temperature up to 800 K, and it was measured by a J-type thermocouple attached to the sample holder. When fast sample cooling was required, water or liquid nitrogen was conducted through the sample cooling loop.

As the positron source, we used the ^{22}Na isotope. A few microCuries of aqueous solution of ^{22}NaCl was dropped onto the sample grains before filling the sample cell completely. By this method the positron source was homogeneously distributed inside the sample.

In the ^{22}Na isotope a 1.28 MeV photon is simultaneously emitted with a positron from the nucleus. This photon serves as the start signal for the positron lifetime. The stop signal is an annihilation photon, emitted when the positron annihilates with an electron. The energy window at the stop side was adjusted to accept photons in the energy range 200−550 keV in order to detect both 2γ and 3γ annihilation of the o-Ps. The intensity observed in the experiments depends on the $3\gamma/2\gamma$ ratio, and thus it is sensitive to the chosen energy window. The γ-photons were measured with two plastic scintillator detectors, the size of which were ϕ 4×4 in. at the start side and ϕ 3×3 in. at the stop side. A lifetime spectrum was obtained by collecting about 10^6 events in the memory of a multichannel analyzer.

The measured lifetime spectra were analyzed by fitting a sum of exponential functions to the data, starting from 7 ns after the zero peak. Thus all the short lifetime components arising from positrons annihilating inside the grains were ignored. The long tail in the lifetime spectrum represents the o-Ps inside the cavities. As a result of fitting, several lifetimes were obtained, but only the average o-Ps lifetime $\tau_{o\text{-}Ps} = \sum I_i\tau_i/\sum I_i$ and the total intensity $I_{o\text{-}Ps} = \sum I_i$ are reported in this work.

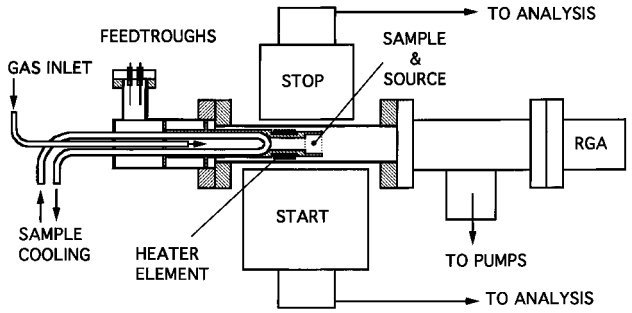

Figure 2. Schematic view of the apparatus. The sample chamber is a 38 mm tube pumped with an oil-diffusion pump. A residual gas analyzer is used for vacuum diagnostics and desorption studies. The positron lifetimes are measured with two scintillator detectors: START adjusted to detect the 1280 keV nuclear γ, emitted at positron emission, and STOP adjusted to detect the 511 keV γ, emitted at positron annihilation.

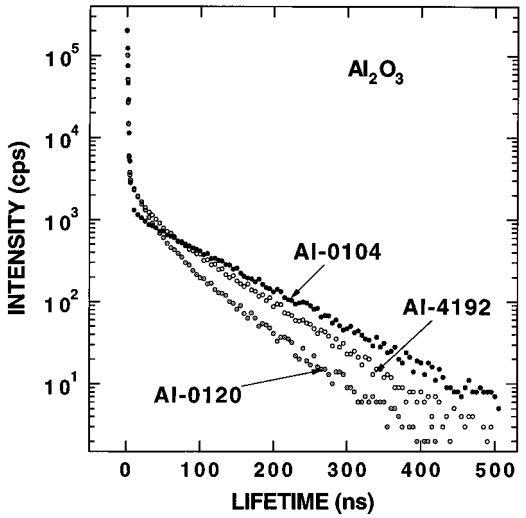

Figure 3. Lifetime spectra of o-Ps in Al-0104, Al-4192, and Al-0120 carriers. The peak at 0 ns is due to positrons annihilating inside the alumina grains. The lifetime spectrum of the Al-0104 carrier is a straight line with one lifetime, whereas the Al-4912 and Al-0120 carriers exhibit a rounder spectrum with several o-Ps lifetimes.

Experimental Results

1. Carrier Materials. Three different alumina carriers of different surface areas and pore size distributions were investigated. The o-Ps lifetimes and intensities in these carriers are given in Table 1. The lifetime spectra of the alumina carriers are shown in Figure 3. The spectrum from the Al-0104 carrier exhibits almost a straight line on the logarithmic scale, indicating only one lifetime component. The shape of the lifetime spectrum from the Al-4912 with 200 m^2/g surface area is more curved and indicates the presence of several long lifetime components. The Al-0120 exhibited an even more curved lifetime spectrum and gave the shortest average lifetime.

On the basis of the form of the lifetime spectra, the Al-0104 material was selected as the carrier for the Pt and Co measurements. This was because the analysis is more straightforward when the spectrum consists of only one lifetime component. A small set of Co and Ni catalysts were, in addition, prepared on the Al-4912 carrier.

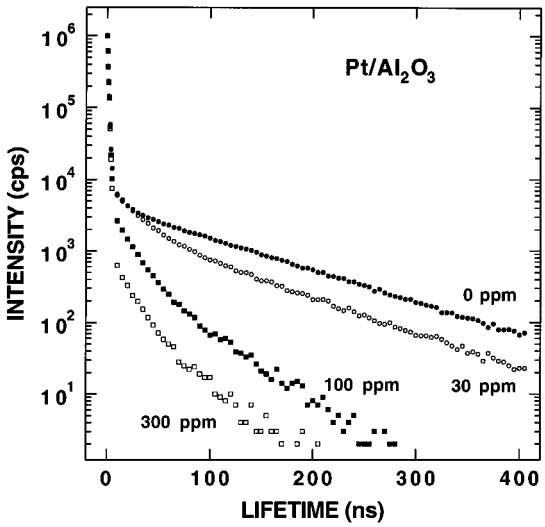

Figure 4. Lifetime spectra of o-Ps in reduced Pt/Al_2O_3 catalysts (Al-0104 carrier). The quenching effect of 3 wt ppm of Pt is already visible. Above 300 wt ppm of Pt no further changes could be observed.

2. The Effect of Metal Loading. The effect of metal loading in the catalyst was studied by adding various amounts of Pt and Co onto the Al-0104 carrier. The effect of Pt on the lifetime spectra is shown in Figure 4 in the concentration range below 300 ppm. As can be seen, only 30 ppm of Pt affects the lifetime spectrum. The 3 and 10 ppm spectra (not shown) are located between the 0 and 30 ppm spectra, but the difference between the 0 and 3 ppm spectra is barely visible. When the concentration exceeds 300 ppm, no more visible changes take place in the lifetime spectra. The o-Ps lifetimes ($\tau_{o\text{-}Ps}$) and intensities ($I_{o\text{-}Ps}$) obtained by fitting a sum of exponential functions to the spectra are given in Table 2. Both of these signals decrease with a concentration increase.

In the case of Co/Al_2O_3, no changes were detected at small concentrations, but only after 1000 ppm the lifetime and the intensity started to decrease, as can be seen in Table 2. The saturation value for the average lifetime was not obtained until 10% concentration. The difference in the absolute level of 0 ppm Pt and Co samples is explained by the different catalyst precursor: The 0 ppm metal-containing samples have passed through the same impregnation−calcination−reduction procedure as those with the metal loading, and some residues can be deposited on the surfaces even in the 0 ppm case.

The annihilation rate $\lambda_{o\text{-}Ps}$ (the inverse of the lifetime) can be expressed as a sum of the annihilation rate of pure carrier λ_o and the chemical quenching rate due to the catalytically active metal of concentration c as[14]

$$\lambda_{o\text{-}Ps} = \lambda_o + k_q c \qquad (1)$$

where k_q is the quenching rate coefficient. The annihilation rate and the o-Ps intensity as a function of Pt concentration on Al-0104 carrier are shown in Figure 5. Both the annihilation rate and the o-Ps intensity saturate before the 300 ppm Pt concentration. The quenching rate coefficient k_q has a value of 350 [at. %]$^{-1}$ ns^{-1} based on the initial slope of the curve up to 100 wt ppm (0.005 at. %). In the case of the cobalt catalyst, the value for k_q was 1.1 [at. %]$^{-1}$ ns^{-1}, and the linearity holds up to the 10^4 wt ppm (1.7 at. %) metal concentration, after which the saturation starts to occur.

Because the difference between the Co and Pt catalysts was remarkable, we also investigated the difference between two transition metal catalysts. Co/Al_2O_3 and Ni/Al_2O_3 samples made on the Al-0120 carrier were compared with each other in the concentration range from 100 to 10 000 wt ppm. The annihilation rate and o-Ps intensity measured from these samples are shown in Figure 6. The behavior of these two systems is very similar in both the o-Ps intensity and the annihilation rate as a function of metal concentration, but the dependence of the annihilation rate on the metal loading is not linear, as was the case with Co on Al-0104. The value of k has an initial value of 41 [at. %]$^{-1}$ ns^{-1} for both metals, but it decreases by 2 orders of magnitude as the metal concentration increases.

TABLE 2: Average Lifetimes and Intensities of o-Ps in Pt/Al_2O_3 and Co/Al_2O_3 Catalysts

concentration (ppm)	Pt		Co	
	$\tau_{o\text{-}Ps}$ (ns)	$I_{o\text{-}Ps}$ (%)	$\tau_{o\text{-}Ps}$ (ns)	$I_{o\text{-}Ps}$ (%)
0	64	11.5	92	20
3	62	9.7		
10	42	9.9	92	20
30	54	8.4		
100	32	2.6	91	20
300	25	0.4		
1000	27	0.3	82	20
2000	28	0.4		
3000	20	0.4		
5000	24	0.4		
7000	24	0.5		
10 000	20	0.5	33	18
100 000			26	17

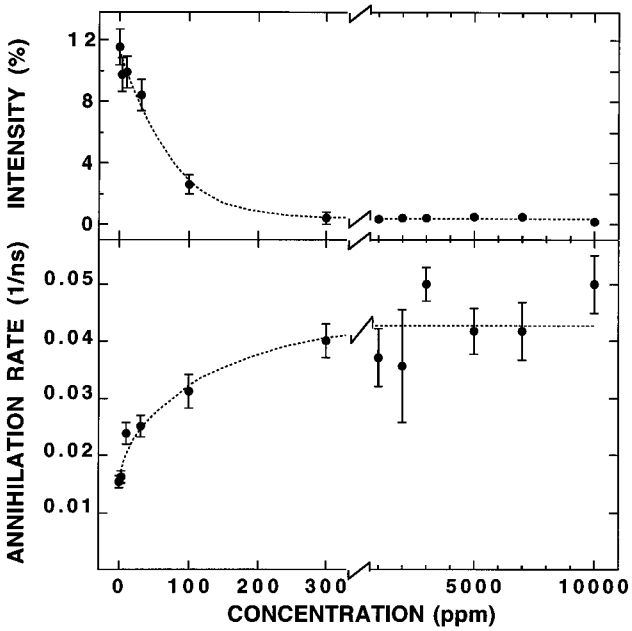

Figure 5. Intensity (above) and annihilation rate (below) of o-Ps in Pt/Al_2O_3 catalyst as a function of Pt loading (wt ppm).

Monte-Carlo Simulations

We have performed Monte-Carlo simulations in order to study the effect of metal atoms on the Ps atom inside the alumina pores. The alumina carrier was described as a set of tubes with a pore size distribution obtained from the data supplied by the manufacturer. The tube diameter was assumed to be constant over the whole length of the tube and the o-Ps atom was assumed to live in only one tube. The probability of the o-Ps entering the tube is proportional to the tube surface area because the o-Ps formation has taken place in the vicinity of the tube. The kinetic energy of the o-Ps was fixed at 25 meV.

Inside the cavity the o-Ps atom collides with the tube wall, and doing so it can either reflect or annihilate. For reflection we assumed that the collision is elastic with no energy losses

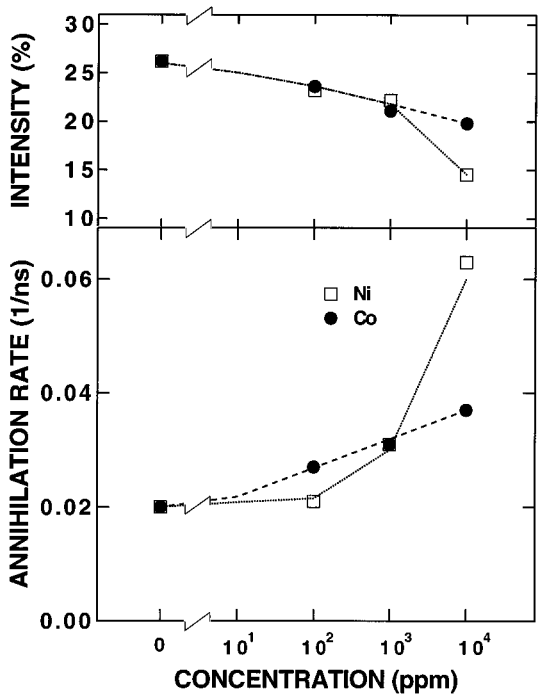

Figure 6. Intensity (above) and annihilation rate (below) of o-Ps in Co/Al_2O_3 and Ni/Al_2O_3 catalysts (Al-0120 carrier) as functions of the metal loading (wt ppm).

and that the collision angle remains constant for all collisions. Recently, it has been reported[15,16] that although the energy of the Ps atom would be as high as 1 eV, thermalization takes place in few nanoseconds via elastic collisions with the wall atoms. However, we decided to keep the calculation as simple as possible and ignored any energy loss process.

The metal atoms deposited on the carrier were assumed to form a monoatomic layer on the inner surfaces of the tubes. The presence of the metal was taken into account by calculating the fraction θ of the pore surface covered with metal atoms and requiring that the same fraction of the Ps atoms collide with the metal particles. The surface atom density of both the carrier and the active metal was approximated with 10^{15} atoms/cm^2. The calculated metal atom coverage is thus proportional to the concentration at low concentration regime. The maximum concentrations used in the simulations were 0.1 wt % Pt and 3.5 wt % Co, corresponding to $\theta_{Pt} = 0.0031$ and $\theta_{Co} = 0.36$. The collisions with the metal areas lead to annihilations with a probability p_{met}. Thus the annihilation probability becomes

$$p = (1 - \theta)p_{carr} + \theta p_{met} \qquad (2)$$

where p_{carr} is the annihilation probability per collision for the carrier material.

The calculation procedure can be summed up as follows: First a tube diameter was randomly selected using the experimental pore size distribution. A lower limit of 5 Å was used so that a new tube was selected until that requirement was satisfied. Then two takeoff angles (polar and azimuthal) were selected, and the time difference between two collisions was calculated. The number of collisions in the tube was calculated using the probability p by randomly drawing it from a Poisson distribution with an expectation value of $1/p$. The lifetime in the tube was then obtained by multiplying these two values.

The Ps lifetime distribution in vacuum, with a mean lifetime of 142 ns, was also taken into account by drawing a random lifetime value with an expectation value of 142 ns. The simulated lifetime was then obtained by comparing the value calculated from the vacuum lifetime distribution to the lifetime in the tube, and the shorter one of these two lifetimes was chosen.

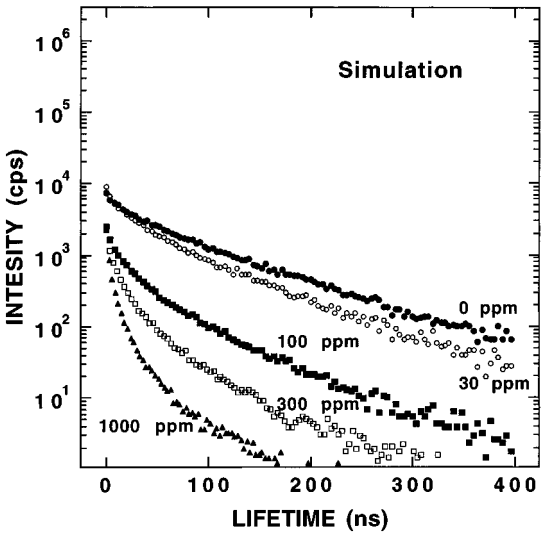

Figure 7. Simulated o-Ps lifetime spectra in Pt/Al_2O_3 catalysts (Al-0104 carrier) with different Pt loadings. The quenching effect of the metal can clearly be seen, and the shortening of the lifetime continues below the experimental limit.

We used in the simulations two carriers, Al-0104 and Al-4192, because the pore size distributions of those were available. The annihilation probability per collision was adjusted in the simulations to give the experimental average o-Ps lifetime, 92 ns for the Al-0104 carrier and 58 ns for the Al-4192 carrier. The corresponding values of p_{carr} were 2×10^{-7} and 7×10^{-7} for the Al-0104 and Al-4192 carrier, respectively. The simulated Ps lifetime spectra agree well with the experimental lifetime spectra in Figure 3. The shape of the lifetime spectrum of the Al-4192 carrier is slightly rounded at short lifetime values, whereas the Al-0104 carrier exhibits more linear behavior, as in the experimental data.

The effect of varying metal concentration in the simulated lifetime spectra was studied in the concentration range of Pt from 1 to 1000 wt ppm on the low surface area Al-0104 carrier. The 1 ppm spectra did not show any difference from the 0 ppm spectra, and even at 10 ppm the changes were barely visible. The simulated spectra in the concentration range from 30 to 1000 ppm are shown in Figure 7. The shortening of the lifetime can be seen during the whole concentration range, even beyond the experimental limit of $\tau_{o\text{-}Ps} \approx 25$ ns. The decrease in the lifetime is similar in the Al-4192 carrier (not shown), and the initial difference in the average lifetime between the carriers gradually disappears when the concentration increases.

The simulated spectra in Figure 7 have been scaled to give the same o-Ps intensity ratios as in the experimental data. This is necessary, because in the simulations all the signal is from o-Ps, but in the experimental data the formation of o-Ps depends strongly on the metal concentration, as can be seen in the upper parts of Figures 5 and 6.

The simulations were repeated also with Co in the concentration range from 3 to 35000 ppm. The simulated spectra were similar to those shown in Figure 7, but the concentration needed to decrease the o-Ps lifetime was 2 orders of magnitude higher than in the case of Pt.

Discussion

1. Carrier Materials. The o-Ps intensity (20%) of the lower surface area (100 m^2/g) carrier, shown in Table 1, is smaller

than that measured in the higher surface area (200 m^2/g) carriers (22−23%). According to Venkateswaran et al.,[17] the Ps intensity in the porous materials is an increasing function of the surface area in the range varying from 30 to 800 m^2/g. The increase in the intensity is explained by the increasing surface to volume ratio, resulting in a higher probability for the positron to escape from the grains to the vacuum.

The overall shape of the lifetime spectra from supports having 200 m^2/g surface area is round, whereas the 100 m^2/g Al-0104 carrier exhibits an almost linear decrease in the spectrum, as shown also in Figure 3. The observed shorter lifetime in the higher surface area carrier is analogous to the curved spectra obtained both experimentally and in the simulations. The shape of the spectra is explained by the pore size distribution of the carrier and is discussed below. The other possible explanation lies with the difference in the annihilation probability per collision used in the simulations. Because in the Al-9120 the annihilation probability is higher, two things occur: The o-Ps in smaller holes annihilates more quickly, producing shorter lifetimes, and thus the larger holes have a more pronounced contribution, giving roundness to the spectrum. The difference in the annihilation probability per collision indicates small differences in the surface compositions of these two carrier materials.

The pore size distributions were available for the Al-0104 and Al-4192 carriers. The normalized pore size distributions of the two carriers are fairly similar, but the total pore volume is 2.5 times larger in the Al-4912 carrier. Half of the pores on both carriers are below 12 nm in diameter, and because of the small volume of these pores, they correspond to the main fraction of the surface areas of the carriers. The main differences between these carriers are in the pore diameter range 12−20 nm, where the Al-4912 carrier has over 20% of its pore volume (compared to 8% in Al-1040), and 0.1−1 μm, where the Al-0104 carrier has about 20% of its pore volume (compared to 12% in Al-4912).

The round shape of the Al-4912 carrier obtained both experimentally and in the simulations is obviously due to the large fraction of 12−20 nm pores, giving rise to a continuous spectrum of lifetimes. On the other hand, the 100 m^2/g surface area support, having a more homogeneous pore size distribution, exhibited a more one-component-like lifetime spectrum.

Using the kinetic energy of 25 meV for o-Ps, one can estimate that in 90 ns an o-Ps travels a distance of 6 mm. For the annihilation probability 2×10^{-7} per collision the average number of collisions would be 5×10^6. Comparing the traveled distance and the average number of collisions, we can see that even 2 nm tubes are large enough to produce quenching rates that are below the o-Ps vacuum annihilation rate, 142 ns^{-1}.

The difference between the 0 ppm Pt and the pure Al-0104 carrier can be explained by the sample preparation method before the Ps experiment. The 0 ppm metal-containing samples have passed through the same impregnation−calcination−reduction procedure as those with the metal loading. This procedure can easily change the surface composition of the carrier. The annihilation probability per collision used in the simulations for the 0 ppm Pt sample was twice that for the clean surface. This change in the annihilation probability corresponds to less than 3 ppm of metallic impurities.

2. The Effect of Metal Loading. The effect of the catalyst metal in the lifetime spectra is shown in Figures 4 and 7 on the Al-0104 carrier. As mentioned earlier, very small amounts of metal can be seen in the lifetime spectrum. The decrease in the lifetime due to metal deposition is explained by the free electrons available in the metal particles with which the o-Ps atom can annihilate via the pick-off process. In the simulated spectra we can see a similar decrease in the lifetime.

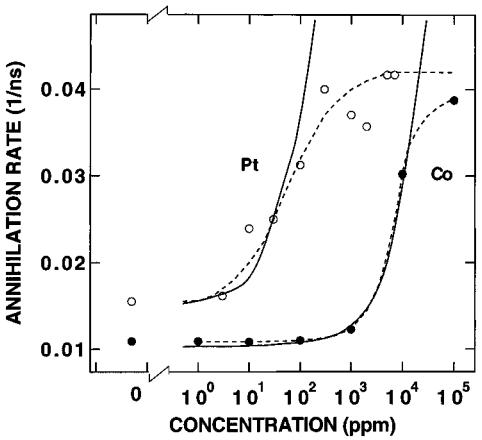

Figure 8. o-Ps annihilation rate as a function of metal loading in alumina. The open circles are the data for the Pt experiments and the filled circles from the Co experiments. The dashed lines are drawn to guide the eye. The solid lines are obtained by simulations using a annihilation probability per collision, p, as the adjustable parameter: For a collision with a Pt-covered area $p_{Pt} = 4 \times 10^{-3}$ and with a Co-covered area $p_{Co} = 1.2 \times 10^{-5}$. The experimental limit of 0.043 ns^{-1} causing the saturation in the Pt and Co data is not taken into account in the simulations.

The experimental lifetime spectra clearly show the presence of several lifetime components, as indicated in the "roundness" of the spectra. This feature gets more pronounced with the increase in the metal concentration. In the simulations, similar features can be seen. Based on the simulations, the following explanation can be given: In the clean support, the annihilation probability for a single collision is very small, resulting in long lifetimes even in the smallest tubes, and in many cases the annihilation is due to the 3γ self-annihilation of o-Ps. When this is the case, the larger tubes cannot produce longer lifetimes and the total lifetime spectrum appears to have only one lifetime component. When the metal concentration increases, the possibility that the o-Ps annihilates prior to self-annihilation increases, and thus the smaller tubes will give shorter lifetimes and the larger tubes longer lifetimes, leading to the roundness of the spectrum.

The annihilation rate results obtained from the Al-0104 carrier are collected in Figure 8. The shape of the measured curves in Pt and Co samples are similar, starting close to the vacuum value of 142 ns^{-1} and saturating to the experimental limit corresponding to ~25 ns^{-1}. The major difference between the curves is in the concentration where the changes in the annihilation rate are observed. The $\lambda_{o\text{-}Ps}$ saturates at a concentration that is 2 orders of magnitude smaller in the case of Pt than in the case of Co. The same information is obtained in the values of the quenching rate coefficient k_q in eq 1 describing the effect of the metal concentration: Its value is $k_q(Pt) = 350$ [at. %]$^{-1}$ ns^{-1} and $k_q(Co) = 1.1$ [at. %]$^{-1}$ ns^{-1}. The values for the quenching rate coefficient have previously been measured in γ-alumina impregnated with, for example, Ni, Co, and Fe nitrate.[10,13] These samples have only been calcined but not reduced, making the comparison with our values difficult. The quenching rate coefficients for Ni and Co are $k_q(Ni) = 1.4$ [at. %]$^{-1}$ ns^{-1} and $k_q(Co) = 0.39$ [at. %]$^{-1}$ ns^{-1},[10] and that for Fe $k_q(Fe) = 2.3$ [at. %]$^{-1}$ ns^{-1} [10] or $k_q(Fe) = 1.0$ [at. %]$^{-1}$ ns^{-1}.[13] Adsorption of air on the surface caused the k_q value to decrease by a factor of 10,[13] indicating that 1 or 2 orders of magnitude difference can really be explained by the state of reduction.

The differences between the Pt and Co catalysts can be explained by the different chemical state and dispersion of the

metal atoms in the reduced catalysts. Pt is mostly metallic after reduction, whereas the less noble Co exists mainly as oxide or aluminate and can not be distinguished from the support material by the o-Ps atoms due to the lack of free electrons. The same effect has been observed in silica-supported iron, where the reduction was seen to decrease and oxidation to increase the lifetime and the intensity of the o-Ps lifetime component.[12]

The experimental results are compared with the simulations in Figure 8, where the solid lines represent the simulated concentration dependencies and the open and filled circles the experimental data. It can be observed that the simulated annihilation rate reproduces well the experimental data below the saturation value. In the simulated data shown in Figure 8 the annihilation probability of the o-Ps atom at the collision with a Pt cluster was $p_{Pt} = 4 \times 10^{-3}$ and with a Co cluster $p_{Co} = 1.2 \times 10^{-5}$. These values give rise to the following thoughts. For the carriers and both metals $p \ll 1$, indicating that the o-Ps reflection probability $(1 - p)$ is very close to 1. This is consistent with the idea that the quantum mechanical reflection approaches 1 at long wavelengths for any particle. The fitted value of $p_{Pt} = 4 \times 10^{-3}$ is 2 orders of magnitude higher than the $p_{Co} = 1.2 \times 10^{-5}$, indicating that Pt is much more reduced than Co in the catalyst. The annihilation probability per collision with the metal cluster can also be compared to the annihilation probability per collision with the support surface. We see that $p_{Co}/p_{carr} \approx 100$ and $p_{Pt}/p_{carr} \approx 10\,000$; that is, the metal-covered surfaces are far more reactive than the carrier surface.

On the basis of the nature of the o-Ps signal we want to make our final comments. The PAS is sensitive to the chemical state of the carrier material surface and senses the difference between oxide and metallic species. Like gas atoms in adsorption and desorption, the o-Ps in sensitive only to the outermost atom layer, and if three-dimensional metal clusters are formed, PAS senses only the cluster surface. The most important difference from the studies performed in gas adsorption is that PAS does not differentiate between pores that are totally closed and those that can be penetrated from outside. This difference can to some extent increase the contribution of small pores in the simulations.

Conclusions

We have shown that o-Ps lifetime spectroscopy is a sensitive tool to measure alumina-supported catalysts. The results indicate that the technique can be used to obtain information on the dispersion and on the chemical state of the catalyst metal. The shape of the lifetime spectrum reflects the pore size distribution of the carrier material.

PAS seems to be very sensitive to reduced Pt, because only 200 ppm is enough to fully saturate the signal. The ultimate sensitivity can be used to measure Pt catalyst deactivation and aging characteristics. In the case of less reducible metals, the method is sensitive in the concentration range used in the industrial catalyst: PAS detects only 0.1% of the Co present in the catalyst. The reason for this is the lower dispersion and higher oxidation of Co on alumina when compared with Pt.

Monte-Carlo simulations can be used to reproduce the experimental o-Ps lifetime spectra and to model quantitatively the behavior of the o-Ps atom in porous media.

Acknowledgment. We thank Mrs. Päivi Mäkinen and Mr. Kim Fallström for their contribution in the positron annihilation experiments. We thank also Mr. Matti Huuska and Mr. Matti Reinikainen from the Chemical Laboratory of the State Research Center of Finland for supplying the catalysts used in these studies. We are grateful for the discussions with Dr. Asko Vehanen, Prof. Outi Krause, and Prof. Veikko Komppa. Financial support from the Technology Development Center and Neste Corporation is acknowledged.

References and Notes

(1) See e.g.: Deviney, M. L.; Gland, J. L., Eds. *Catalyst Characterization Science*; ACS Symposium Series 288; American Chemical Society: Washington, DC, 1985.

(2) Hautojärvi, P., Ed. *Positrons in Solids*; Topics in Current Physics, Vol. 12; Springer: Berlin, 1979.

(3) Dupasquier, A.; Mills, A. P., Jr., Eds. *Positron Spectroscopy of Solids*; IOS Press: Amsterdam, 1995.

(4) Lahtinen, J.; Vehanen, A. *Catal. Lett.* **1991**, *8*, 67.

(5) Cheng, K. L.; Jean, Y. C.; Luo, X. H. *Crit. Rev. Anal. Chem.* **1989**, *21*, 209.

(6) Schrader, D. M.; Jean, Y. C., Eds. *Positron and Positronium Chemistry*; Studies in Physical and Theoretical Chemistry, Vol. 57; Elsevier: Amsterdam, 1988.

(7) Ito, Y.; Takano, T.; Hasegawa, M. *Appl. Phys. A* **1988**, *45*, 193; **1990**, *50*, 39.

(8) Huang, W. F.; Huang, D. C.; Tseng, P. K. *Catal. Lett.* **1994**, *26*, 269.

(9) Venkateswaran, K.; Cheng, K. L.; Jean, Y. C. *Chem. Phys. Lett.* **1986**, *126*, 33.

(10) Lou, X. L.; Cheng, K. L.; Jean, Y. C. In *Positron Annihilation*; Jain, P. C., Singru, R. M., Gopinathan, K. P., Eds.; World Scientific: Singapore, 1985.

(11) Kobayashi, Y.; Takeuchi, K. *Mater. Sci. Forum* **1995**, *175*−*178*, 703.

(12) Mogensen, O. E.; Eldrup, M.; Mørup, S.; Ørnbo, J. W.; Topsøe, H. In *Positron Annihilation*; Jain, P. C., Singru, R. M., Gopinathan, K. P., Eds.; World Scientific: Singapore, 1985.

(13) Lévay, L.; Takashima, Y.; Kuramoto, E.; Juhász, J.; Lévay, B.; Vértes, A. *Mater. Sci. Forum* **1992**, *105*−*110*, 1633.

(14) Venkateswaran, K.; Cheng, K. L.; Jean, Y. C. *J. Phys. Chem.* **1985**, *89*, 3001.

(15) Nagashima, Y.; Kakimoto, M.; Hyodo, T.; Fujiwara, K.; Ichimura, A.; Chang, T.; Deng, J.; Akahane, T.; Chiba, T.; Suzuki, K.; McKee, B. T. A.; Stewart, A. T. *Phys. Rev. A* **1995**, *52*, 258.

(16) Dauwe, C.; Consolati, G.; van Hoecke, T.; Seegers, D. *Nucl. Instrum. Meth. A* **1996**, *371*, 497.

(17) Venkateswaran, K.; Cheng, K. L.; Jean, Y. C. *J. Phys. Chem.* **1984**, *88*, 2465.